Scientific paper

# Carbon-Paste Electrode Modified by $\beta$ -Cyclodextrin as Sensor for Determination of Sunset Yellow FCF and Ponceau 4R in Soft Drinks

#### Konstantin Pliuta and Denys Snigur\*

Department of Analytical and Toxicological Chemistry, Faculty of Chemistry and Pharmacy, Odesa I.I. Mechnikov National University, Odesa, 65082, Ukraine

\* Corresponding author: E-mail: 270892denis@gmail.com

Received: 07-18-2022

#### **Abstract**

One of the disadvantages of voltammetric analysis is the significant amount of sample required for electrolysis in the cell. In this paper a methodology close to adsorption stripping voltammetry was proposed to solve this problem at an analysis of two azo dyes – Sunset Yellow FCF and Ponceau 4R. As a working electrode, a carbon-paste electrode modified with  $\beta$ -cyclodextrin, a cyclic oligosaccharide that can form supramolecular complexes with azo dyes was proposed. The redox behavior of Sunset Yellow FCF and Ponceau 4R, the number of electrons, protons, and charge transfer coefficients onto the proposed sensor have been studied. Using square-wave voltammetry, the conditions for the determination of two dyes were optimized. Under the optimal conditions the calibration plots are linear in the ranges 71–565  $\mu$ g/L and 189–3024  $\mu$ g/L for Sunset Yellow FCF and Ponceau 4R, respectively. Finaly, the new sensor has been tested for square-wave voltammetric determination of Sunset Yellow FCF and Ponceau 4R in soft drinks, and RSD values (max. 7.8 and 8.1%) indicated satisfactory precision for both analyzed samples.

**Keywords:** Voltammetry, carbon-paste electrode, food azo dyes,  $\beta$ -cyclodextrin, azo dyes.

#### 1. Introduction

Sunset Yellow FCF (SY, E110) and Ponceau 4P (P4R, E124) belong to the class of sulfonated azo dyes that are widely used today in the food and pharmaceutical industries. WHO allows the use of these dyes in various food and pharmaceutical products with an acceptable daily intake of 4 mg/kg of body weight.<sup>2</sup> As with other similar food azo dyes, EFSA conducted studies on the possible toxicity of SY and P4R<sup>3</sup> and concluded that these dyes do not have a mutagenic and carcinogenic effect, and do not harm human health when consumed within the established limits by WHO. However, there is a different opinion in the scientific community involved in research on the effects of food azo dyes. Thus, several researchers argue that prolonged use of such dyes as SY and P4R can lead to damage to liver and kidney cells, 4,5 as well as an increase in oxidative stress of lipids in various tissues.<sup>4</sup> A similar effect is exerted by other food azo dyes similar in structure, such as tartrazine, carmoisine, and Allura Red.<sup>6,7</sup>

Over the past 20 years, many electrochemical sensors have been proposed for the determination of food azo

dyes.8-10 To increase the sensitivity and selectivity of sensors, various modifiers were used, such as carbon nanomaterials, 11 metal nanoparticles and their oxides, 12 polymeric materials, 13 and others. 14 Most often, both carbon paste 15-17 and glassy carbon electrodes<sup>18</sup> were used for sensor bases, like other types of electrodes. 19 However, in most cases the voltammetric determination was accompanied by some disadvantages – a significant amount of supporting electrolyte solution to fill the electrolytic cell for electrolysis. Standard electrochemical cell is designed for 15-25 mL of sample for electrolysis.<sup>20</sup> To solve this problem, either low-capacity cells with small electrodes or an alternative method of electrolysis are required. In this work, a methodology close to adsorptive stripping voltammetry was proposed. The single drop methodology can be represented as follows: a small amount of sample (10 µL) is pipetted onto the modified electrode surface and is kept a certain time for the sorption stage, after which the electrode is rinsed and electrolysis is carried out in a pure buffer solution.

β-Cyclodextrin (β-CD) is a cyclic oligosaccharide in which 7 molecules of glucopyranose are linked by α-(1,4) bond. The production of β-CD is based on the enzymatic

breakdown of starch, and today it is produced on an industrial scale. <sup>21</sup> Cyclodextrins are widely used in the food and pharmaceutical industries and are also often used to create sensors for various purposes. <sup>22</sup>  $\beta$ -CD is also used to create sorbents for the various azo dyes removal. <sup>23,24</sup> The ability of  $\beta$ -CD to form supramolecular inclusion complexes with azo dyes, <sup>25,26</sup> and its inexpensiveness make it a promising sorption modifier for working electrodes.

The current study is aimed to investigate the possibility of voltammetric determination of SY and P4R using carbon-paste electrode modified by  $\beta\text{-CD}$  (CPE/ $\beta\text{-CD}$ ) from one drop. The usage of  $\beta\text{-CD}$  as modifier that improves the sorption affinity of the carbon-paste electrode surface opens up the possibility of implementing the "single-drop method". Thus, it is possible to accumulate analytes on the sensor surface from a small volume of liquid (10  $\mu\text{L})$  – one drop.

#### 2. Experimental

#### 2. 1. Reagents and Apparatus

SY, P4R, silicone oil and  $\beta$ -CD were obtained from Merck (Germany). Carbon C1 grade with a particle size of  $\leq$ 15 µm (UkrSpecMasla, Ukraine) was used for the preparation of carbon-paste electrode. Double distilled water was used to prepare standard and buffer solutions, as well as to rinse the electrode.

Voltammograms were recorded using an Ecotest VA potentiostat (Econiks Expert, Russia) equipped with an auxiliary platinum electrode, a silver chloride reference

electrode, and a working CPE/ $\beta$ -CD electrode. The pH was monitored using an I-500 pH-meter (LLC Akvilon, Russia), coupled with a glass electrode.

The Shimadzu Prominence liquid chromatograph, which consists of a pump (LC-20), autosampler (SIL-20), column oven (CTO-20) and spectrophotometric detector (SPD-20), was used to determine food azo dyes in various samples by HPLC. Nucleodur C18ec (length 250 mm, i.d. 4.6 mm and particle size 5  $\mu$ m) was used as an analytical column for the separation of azo dyes.

#### 2. 2. Preparation of CPE/β-CD

For the preparation of carbon-paste, the carbon powder,  $\beta$ -CD, and silicone oil were thoroughly mixed in a mortar until a homogeneous paste was formed. The constant ratio of dry matter to the binder was maintained as 2.3:1 (by weight) in all prepared electrodes. An unmodified electrode was prepared in the same way but without  $\beta$ -CD. As the electrode body, a Teflon tube with an inner diameter of 3 mm was used. For the contact of the carbon-paste electrode with the output of the potentiostat the copper wire was used. The electrode surface was refreshed before each measurement by squeezing out a small portion of the paste, cutting off, and polishing on a piece of weighing paper.

### 2. 3. Determination of Azo Dyes in Soft Drinks

For the soft drinks degassing, a small portion ( $\sim$ 10 mL) was heated to 45 °C and sonicated for 15 min. If nec-

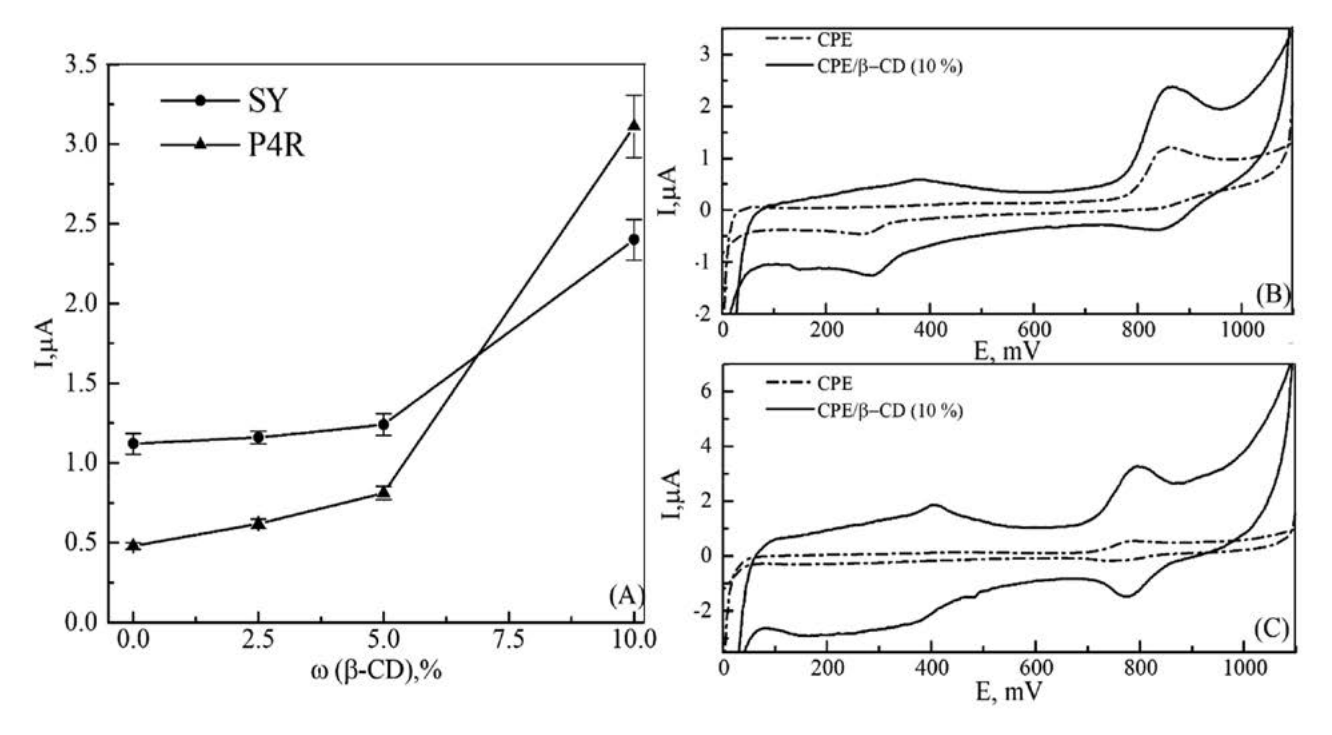


Fig. 1. (A) The plot of oxidation current of dyes as a function of β-CD content in CPE. Cyclic voltammogram of a bare CPE and CPE/ β-CD in a supporting electrolyte (pH = 2) after accumulation of (B) SY (100  $\mu$ M) and (C) P4R (100  $\mu$ M) onto electrode surface from one drop of dyes solution.

essary, the sample was filtered through a hydrophilic PTFE filter. The sample aliquot was transferred in a 5 ml flask and diluted to the mark with a Britton-Robinson buffer solution with pH 2. For single drop methodology procedure,  $10~\mu L$  of the analyzed sample was pipetted onto the sensor surface and held for 5 min, after which the electrode was gently rinsed with double distilled water. A square wave voltammetry ( $\Delta E = 50~\text{mV}$ , f = 15 Hz,  $t_{\text{ads}} = 5~\text{min}$ ) was used for signal registration at a scan rate of 25 mV/s from 300~mV to 1100~mV. Quantitative analysis was carried out according to the standard addition method.

#### 3. Results and Discussion

#### 3. 1. Optimization of Sensor Composition

For the first time the optimal content of the modifier in the working electrode was established. A series of sensors with different contents of  $\beta\text{-CD}$  (from 2.5 to 10 wt. %) was fabricated. One drop (10  $\mu\text{L})$  of the working solution of dyes was pipetted onto the sensor surface and kept for 3 min for sorption. After that, the electrode was rinsed and electrolysis was carried out in a pure buffer solution (pH 2). Oxidation current of dyes was used as a signal for optimal sensor composition (Fig. 1).

As can be seen, with an increase in the content of the modifier, the oxidation currents for both dyes increase and reach maxima at 10 wt %  $\beta\text{-CD}$  in the electrode. This behavior confirms that  $\beta\text{-CD}$  promotes the sorption of dyes on the sensor surface. With a further increase of the  $\beta\text{-CD}$  content, a carbon paste that was difficult to work with was obtained. Therefore, 10 wt.% of  $\beta\text{-CD}$  was chosen as optimal modifier content.

To evaluate the effect of β-CD on the CPE conductive properties, cyclic voltammograms (CV) of a solution of potassium ferrocyanide (1 mM) in 0.1 M potassium chloride on both CPE/β-CD and bare CPE (Fig. S1) were recorded. As can be seen from Fig. S1, the ferrocyanide oxidation and reduction currents on CPE/β-CD were increased compared to bare CPE. The difference between the ferrocyanide oxidation and reduction peak potential ( $\Delta E_p$ ) for bare CPE is 85 mV, while for CPE/β-CD it is 70 mV, which indicates a higher electrocatalytic activity of the modified sensor. The Randles–Sevcik equation was used to determine the CPE/β-CD active area (Equation 1).

$$I_p = (2.69 \cdot 10^5) n^{3/2} A D_{red}^{1/2} v^{1/2} C_{red}^0$$
 (1)

where  $I_p$  – current in amperes, n – number of electrons in the redox reaction, A – the electrode surface area in cm<sup>2</sup>,  $D_{red}$  – diffusion coefficient in cm<sup>2</sup>/s ( $D([Fe(CN)_6]^{4-}) = 7.6 \cdot 10^{-6} \text{ cm}^2/\text{s}^{27})$ , v –scan rate in V/s,  $C_{red}^0$  – concentration in mol/cm<sup>3</sup>.

Using the equation above, the active surface area for CPE/ $\beta$ -CD can be calculated as 0.105 cm<sup>2</sup>, which is ~1.2-times that of bare CPE (0.090 cm<sup>2</sup>). Thus, an increase in the active surface area, as well as a lower value of  $\Delta E_p$  in the case of CPE/ $\beta$ -CD, indicates an increase in the electron transfer rate from the electrode surface.

#### 3. 2. Electrochemical Behavior of Sunset Yellow FCF and Ponceau 4R on the CPE/β-CD Sensor

The suggested methodology was applied to study the redox behavior of SY and P4R on the proposed sensor. To carry out these experiments, after the stage of dye sorption from the solution by the electrode surface, a series of CVs in pure buffer solutions were recorded under different conditions.

#### pH effect

It is known that the pH of a buffer solution strongly affects the protolytic state of dyes in the solution<sup>28</sup> and, consequently, their sorption equilibrium.<sup>29</sup> Using the suggesting methodology, it is possible to carry out sorption and electrolysis at different pH values of the buffer solution, which gives a much greater possibility of the analysis conditions optimization. The influence of buffer solution pH on dyes sorption ability onto the electrode surface and the electrolysis current were investigated (Fig. 2).

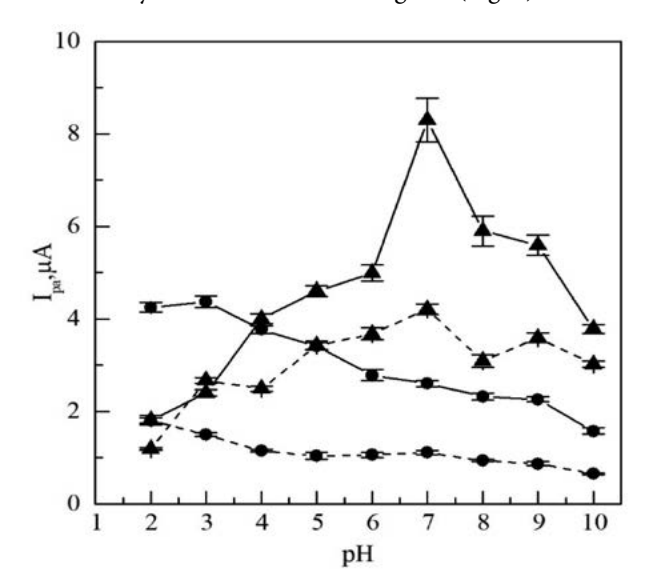


**Fig. 2.** The plot of the oxidation peak current as a function of pH-dependent adsorption for SY (circles, solid line) and P4R (circles, dashed line) and as a function of pH-dependent electrolysis for SY (triangle, solid line) and P4R (triangle, dashed line) onto CPE/β-CD.

In the case of sorption ability increase, buffer solution pH decreases the oxidation current, which indicates the decrease of sorption of dyes onto the sensor surface. This can be explained by the specificity of the formation of

inclusion complexes between dyes and β-CD. The mechanism of formation of complexes between azo dyes and β-CD can include both supramolecular and electrostatic interactions.<sup>30</sup> It should be also noted that azo dyes can interact with the electrode surface both due to  $\pi$ - $\pi$  interactions and via electrostatic forces between carboxyl/ carbonyl groups, which are always present on the surface of the carbon-paste electrode.<sup>31</sup> According to the data of protolytic equilibria of SY and P4R, the lowest degree of ionization of dye molecules is observed in an acidic medium. Given what follows, it can be assumed that, along with supramolecular and electrostatic forces on the modified electrode play an important role in the ability to form inclusion complexes between dyes and β-CD. The pH shift to the alkaline zone increases the ionization of dyes, which may increase their electrostatic repulsions from the electrode surface. As a result, there may be less inclusion complex formation, which will result in lower dye oxidation currents.

The oxidation current of SY and P4R increased at pH 6-7 in the case of the effect of buffer solution pH on electrolysis. At pH > 7, a decrease in the oxidation current was observed for both SY and P4R. In our further studies, pH 2 for the adsorption of dyes and pH 7 for carrying out of electrolysis were chosen.

With an increase in the pH of the supporting electrolyte, the potentials of the oxidation and reduction peaks of dyes shift to the cathodic region (Fig. S2A and S3A), which indicates the participation of the proton in the electrochemical processes. To determine the ratio of protons to electrons (m/n), the dependences of the potentials of the oxidation/reduction peaks ( $E_{\rm pa}/E_{\rm pc}$ ) on the pH (Fig. S2B and S3B) were studied. The following linear equations were obtained for SY:  $E_{\rm pa}(I_{\rm ox}) = -34.2 \, {\rm pH} + 944.4$  and  $E_{\rm pc}(I_{\rm red}) = -32.0 \, {\rm pH} + 922.0$ , and for P4R:  $E_{\rm pa}(I_{\rm ox}) = -31.5 \, {\rm pH} + 860.1$  and  $E_{\rm pc}(I_{\rm red}) = -33.8 \, {\rm pH} + 854.6$ . Thus, based on the values of slopes of the obtained equations in the oxidation/reduction processes, the ratio m/n is 1:2 for both SY and P4R.  $^{20,32}$ 

#### Scan rate effect

For investigation of the nature of the oxidation/reduction current and to establish the number of electrons involved in the redox processes, the CVs of dyes solutions on CPE/ $\beta$ -CD at different scan rates were recorded (Fig. S4).

Based on the obtained data, the dependences of the dyes oxidation current on the scan rate were plotted (Fig. S4C) and can be expressed by the following equations:  $I_{\rm pa}({\rm SY}) = 0.076{\rm v} + 2.34~({\rm R}^2 = 0.997),~I_{\rm pa}({\rm P4R}) = 0.032{\rm v} + 2.39~({\rm R}^2 = 0.995)$ . The linear dependences of the oxidation current on the scan rate indicates the adsorption nature of the dyes oxidation current on CPE/ $\beta$ -CD.  $^{20,32}$ 

Laviron model was used for the determination the number of electrons (n) and the charge transfer coefficient ( $\alpha$ ) involved in the redox processes (Equation 2 and 3).<sup>33</sup>

For this, the dependences between the dyes oxidation/ reduction peak potential ( $E_{pa}/E_{pc}$ ) and the decimal logarithm of the scan rate were constructed (Fig. S5). Using the slope of obtained lines and equations 2 and 3 the n and  $\alpha$  were calculated as: for SY:  $n = 2.16 \approx 2$  and  $\alpha = 0.62$ , and for P4R:  $n = 2.05 \approx 2$  and  $\alpha = 0.56$ . Taking into account the obtained experimental data it can be concluded that two electrons and one proton are involved in the process of oxidation and reduction of SY and P4R onto the CPE/ $\beta$ -CD.

$$E_{pa} = \frac{2.3RT}{(1-\alpha)nF} \cdot lg \, v + const \tag{2}$$

$$E_{pc} = \frac{-2.3RT}{\alpha nF} \cdot lg \, v + const \tag{3}$$

Thus, SY and P4R can be reversibly oxidized on the surface of the proposed sensor. However, it should be noted that the dye oxidation peak current ( $I_{ox}$ ) is much higher than the corresponding reduction current ( $I_{red}$ ). According to Wopschall and Shain,<sup>34</sup> this behavior may indicate the presence of an irreversible chemical reaction with an oxidation intermediate. To confirm this assumption, the ratio of the reduction current ( $I_{red}$ ) to the oxidation current ( $I_{ox}$ ) was plotted for both dyes as a function of the scan rate ( $I_{red}/I_{ox} = f(v)$ ) (Fig. S6). As can be seen, as the sweep rate increases, the ratio between the reduction and oxidation currents for both dyes decrease. This confirms that the process of oxidation of SY and P4R proceeds with the participation of an irreversible chemical reaction (EC<sub>ir</sub> mechanism).

#### Cyclic voltammetry profile

CVs at different numbers of cycles were recorded and thoroughly examined to gain a better knowledge of the mechanism of dyes oxidation.

For two dyes in the first scan cycle, one oxidation peak  $I_{ox}$  (SY:  $E_p(I_{ox}) = 880$  mV; pH = 2, P4R:  $E_p(I_{ox}) = 764$ mV; pH = 3) and the corresponding reduction peak  $I_{red}$ (SY:  $E_p(I_{ox}) = 862 \text{ mV}$ ; pH = 2, P4R:  $E_p(I_{ox}) = 751 \text{ mV}$ ; pH = 3) were observed (Fig. 3). The presence of the corresponding oxidation/reduction peaks is confirmed by many authors, \$\bar{3}5,36\$ which can be attributed to both the oxidation of the azo group and the hydroxyl group located in the naphthalene ring.<sup>37</sup> Also, on the CV of dyes, there is an irreversible reduction peak  $I'_{red}$  (SY:  $E_p(I'_{red}) = 58$  mV; pH = 2, P4R:  $E_p(I'_{red})$  = -131 mV; pH = 3), which refers to the destructive reduction of the azo group to corresponding amines.<sup>38</sup> As can be seen from Fig. 3, in an acidic medium, there is no  $I_{ox}$  oxidation peak for both dyes upon potential reverse scan cycle. This can be explained by the specificity of the measurement according to the suggested methodology. During the first scan cycle, dyes are almost completely irreversibly oxidized at the electrode surface. However, as can be seen in the neutral medium (Fig. 3 inset), there are insignificant dye oxidation peaks in the second scan cycle, which most likely indicate much greater stability of

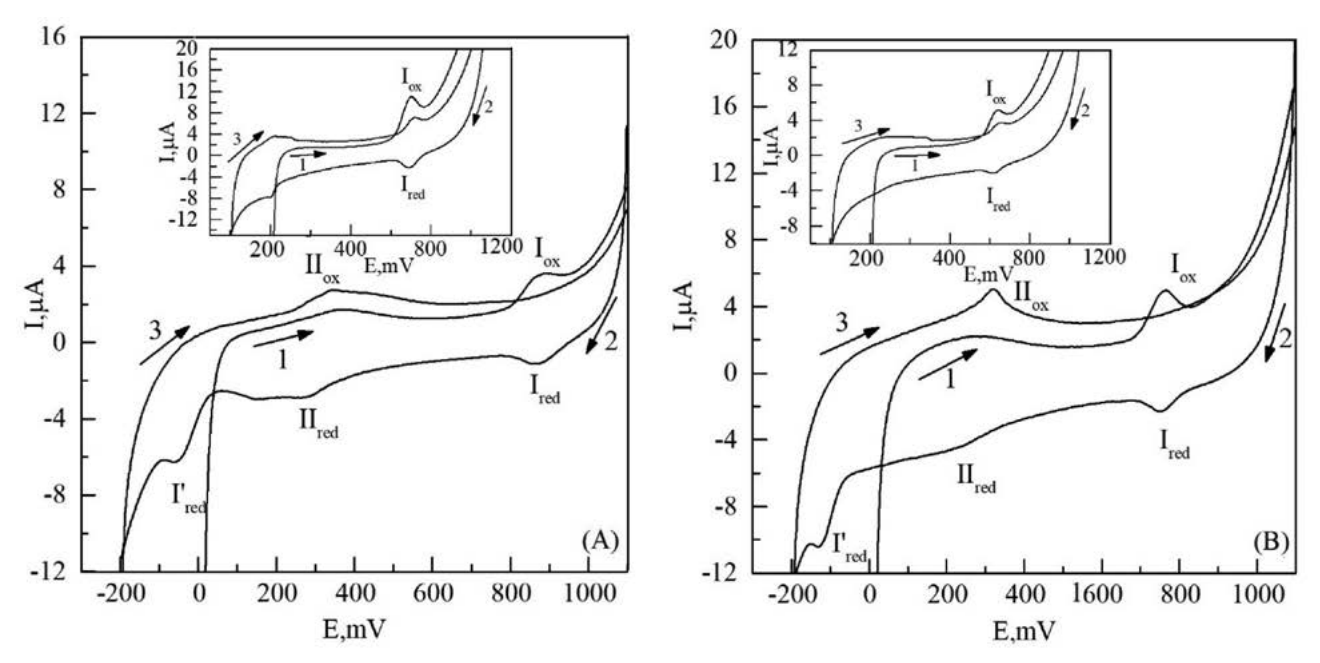


Fig. 3. (A) CV of a buffer solution with pH 2 and pH 7 (insert (A)) onto CPE/ $\beta$ -CD after adsorption on the surface of a solution (10  $\mu$ l) of SY with a concentration of 100  $\mu$ M for 3 min. (B) CV of a buffer solution with pH 3 and pH 7 (insert (B)) onto CPE/ $\beta$ -CD after adsorption on its surface of a solution (10  $\mu$ l) of P4R with a concentration of 100  $\mu$ M for 3 min. Arrows and numbers indicate the direction and order of potential sweep.

the intermediate oxidation products of these dyes in the neutral medium. This, in turn, makes it possible to partially restore the oxidized form of the dye, which is expressed in insignificant oxidation peaks during the subsequent potential sweep (direction  $N^{\circ}$  3 in Fig. 3).

It should be noted that in both cases of SY and P4R, the appearance of a new redox pair  $II_{\rm red}$  (SY:  $E_{\rm p}(II_{\rm red})$  = 284 mV; pH = 2, P4R:  $E_{\rm p}(II_{\rm red})$  = 241 mV; pH = 3) and  $II_{\rm ox}$  (SY:  $E_{\rm p}(II_{\rm ox})$  = 343 mV; pH = 2, P4R:  $E_{\rm p}(II_{\rm ox})$  = 321 mV; pH = 3) after dyes oxidation process in next sweep cycles, which may be related to the oxidative destruction of dye molecules. The appearance of a new redox pair after the oxidation process was also noted by researchers studying the mechanisms of oxidation in partially sulfonated 39 and fully nonsulfonated azo dyes. 40 In both cases, the authors 39,40 noted that the new redox peaks belong to the fragments formed after the oxidative degradation of the molecule.

In this regard, the question was raised about the similarity of the behavior during the reduction of dyes at the azo group. To do this, a series of CVs were recorded with a separate process of oxidation and reduction of dyes to prove the presence of a common redox pair in both oxidative and reductive destruction products (Fig. S7). After the oxidation process and the accumulation of oxidation products, the first and second cycles of the  $II_{\rm ox}$ – $II_{\rm red}$  redox-pare potential range coincide (Fig. S7). In the case of preliminary reduction of azo dyes, the first and second scan cycles in the potential range of the  $II_{\rm ox}$ – $II_{\rm red}$  pair do not coincide. Thus, in the first cycle, the oxidation potential of  $III_{\rm ox}$  is shifted relative to  $II_{\rm ox}$  by 62 mV for SY and by 26 mV for P4R to the anode region. The second cycle

after the pre-reduction process completely coincides with the first and second cycles after the pre-oxidation of the dye. This behavior can be explained by the presence of the azo dyes' reduction products intermediates and the requirement of higher energy for the oxidation of this form, which causes a small shift in the potential of the oxidation peak of  $III_{\rm ox}$  relative to  $II_{\rm ox}$ .

Thus, during the reduction of dyes, new redox pairs also appear, coinciding with the redox pair formed during its oxidation. Consequently, the products of oxidative and reductive destruction of azo dyes have a common redox pair.

In conclusion, it was assumed that a significant disproportion between the currents of oxidation and reduction of azo dyes in the first cycle  $(I_{ox}-I_{red})$  indicates the predominant oxidative degradation of the dyes' molecules under the conditions of signal recording. The destruction of the molecule can be associated with the oxidation process by the EC<sub>ir</sub> mechanism, in which the subsequent chemical reaction can lead to a rearrangement of bonds in the molecule and, as a consequence, to the cleavage of the azo group.<sup>32</sup> Also based on the obtained CV of dye solutions at various scan rates (Fig. S4), it can be concluded that P4R has a more stable oxidation intermediate than SY. This may be evidenced by the presence of a reversible reduction peak in P4R at a minimum scan rate (25 mV/s) in comparison with SY. Thus, at low scan rates for SY, the rate of the subsequent irreversible chemical reaction begins to strongly dominate, which is expressed in the absence of the reduction peak according to  $I_{ox}$ . It was supposed that the match stability of the intermediate oxidation product of P4R is realized due to the compen-

Scheme 1. Suggested mechanism of SY and P4R oxidation onto CPE/β-CD

sation of the excess positive charge in the molecule after the oxidation process. For example, it can be implemented due to the negative charge of the sulfo group located in the peri-position to the azo group. The formation of new redox pairs after the first potential sweep cycle can also confirm our assumption about the oxidative degradation of the molecule due to an irreversible chemical reaction with intermediate oxidation products that produce new electroactive fragments:

## 3. 3. Optimization of Dyes Determination Parameters on CPE/β-CD Sensor

Square wave voltammetry coupled with suggested single drop methodology on the developed CPE/ $\beta$ -CD sensor for the determination of dyes was used. Such typical parameters as potential amplitude ( $\Delta E$ ), frequency (f),

accumulation time ( $t_{ads}$ ) and potential sweep rate (v) were chosen for optimization (Fig. S8, S9).

At increasing potential amplitude and frequency, the resulting current also increased, respectively. The 50 mV and 15 Hz were chosen as the optimal values for the determination of dyes. This is due to the fact that with a subsequent increase in amplitude and frequency, the shape of the peak was strongly distorted (Fig. S8, S9A,B). When investigating the effect of accumulation time, the resulting current plateaus after 5 min for both dyes (Fig. S8, S9B). At increasing scan rate from 25 mV/s to 200 mV/s, a decrease in peak current was observed and less and less clearly identified peak. Probably, this effect arises due to the combination of the registration signal by the suggested methodology with the peculiarity of the potential change in square-wave voltammetry. The optimal scan rate of 25 mV/s was chosen for both dyes.

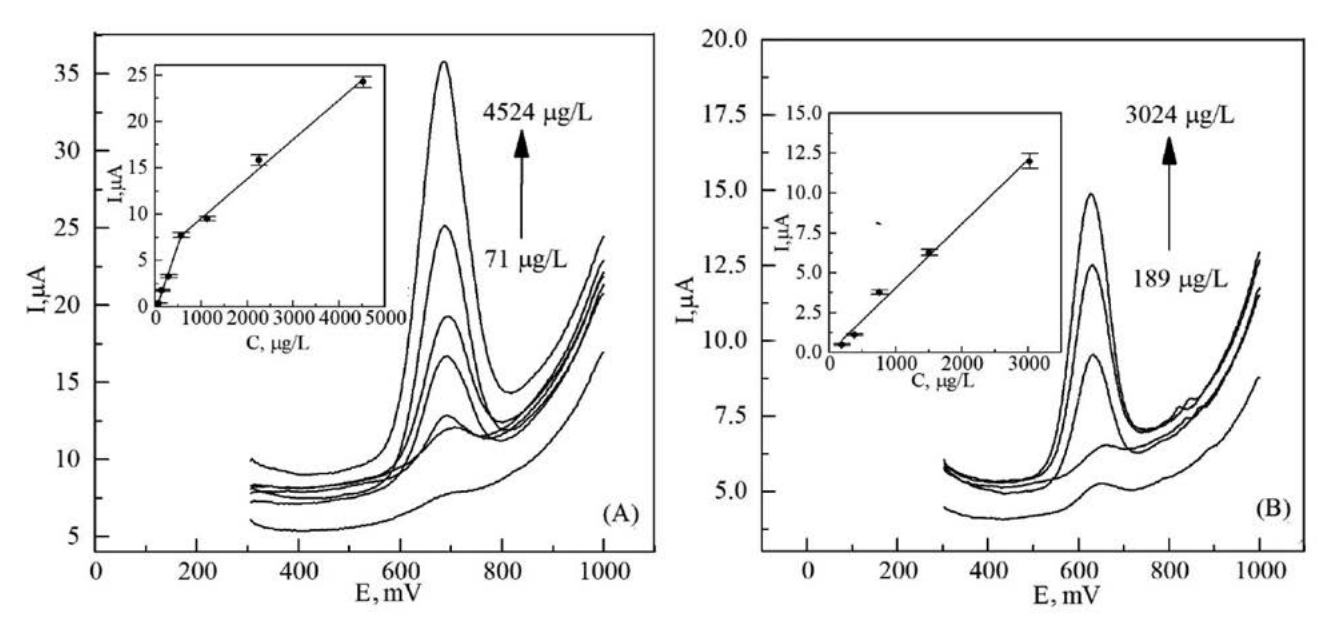


Fig. 4. Square-wave voltammograms of (A) SY and (B) P4R solution for various concentrations. Inserts: plots of the peak currents as a function of concentration.

## 3. 4. Determination of Sunset Yellow FCF and Ponceau 4R on CPE/β-CD in Real Samples

Under the optimal conditions, calibration curves for dyes' determination via proposed method were plotted (Fig. 4).

The obtained calibration curve for SY has two linear sections: 71-565 µg/L and 565-4524 µg/L, which are described by the equations  $I_{pa}(SY) = 14.4C(SY) + 0.59 \pm$  $0.14 (R^2 = 0.993)$  and  $I_p(SY) = 4.3C(SY) + 5.09 \pm 0.81 (R^2 =$ 0.995), respectively. For P4R, the calibration curve is linear in the concentration range 189-3024 µg/L and is described by the equation  $I_p(P4R) = 13.2C(P4R) + 0.59 \pm 0.148$  (R<sup>2</sup> = 0.990). According to the 3σ and 6σ approach,<sup>41</sup> LOD and LOQ for dyes were calculated using data from 6 parallel measurements of SY and P4R solutions at concentrations of 71 and 189  $\mu$ g/L, respectively. The calculated values were for SY: LOD = 42  $\mu$ g/L, LOQ = 85  $\mu$ g/L; and for P4R: LOD = 102  $\mu$ g/L, LOQ = 204  $\mu$ g/L. The proposed sensor was tested on model solutions and soft drinks samples that do not contain dyes. The results of analyses are presented in Table 1.

To test the developed sensor, soft drinks samples were analyzed according to proposed method and via HPLC as a reference method. A description of the HPLC determination method is provided in the Supplementary Materials. Fisher's F-test and Student's and Welch's t-test were used to compare the determination results obtained via the two methods (Table S1).<sup>42</sup> As can be seen from Table S1, the obtained t-statistic values are less than the critical value, which indicates that there is no statistical difference between the results obtained by HPLC and the proposed voltammetric method. According to the obtained results, it can be concluded that the proposed sensor and suggested methodology proved to be satisfactory in the analysis of SY and P4R in soft drinks samples with RSD no more than 8%.

#### 4. Conclusions

In this work, CPE/β-CD for the SY and P4R determination was proposed. Using CV, the influence of supporting electrolyte's pH, as well as the potential sweep rate was studied. It has been established that SY and P4R are oxidized quasi-reversibly with the participation of one proton and two electrons. For both dyes, the formation of a new redox pair was noted in subsequent potential sweep cycles. Based on the obtained data, it was concluded that the oxidation of SY and P4R onto CPE/β-CD occurs with the participation of an irreversible chemical reaction that leads to cleavage of dyes' molecules at the azo group, creating new electroactive piece (the corresponding dyes oxidation scheme was proposed). Using a single drop methodology, a lowering in the minimum amount of sample required for analysis to 10 µL was achieved. Suggested methodology and developed CPE/β-CD sensor was successfully tested at dyes determination in real soft drinks samples with a recovery ratio of 95% and RSD no more than 8%.

#### **Conflicts of interest**

There are no conflicts to declare

#### 5. References

- 1 D. Villaño, C. García-Viguera and P. Mena, *Encycl. Food Heal.*, **2015**, 265–272.
  - **DOI:**10.1016/B978-0-12-384947-2.00190-2
- 2 World Health Organization, *WHO* Technical Report Series: Evaluation of certain food additives and contaminants, **2011**.
- 3 E. Food and S. Authority, EFSA J., 2015, 13, 1-35.
- 4 L. I. Khayyat, A. E. Essawy, J. M. Sorour and A. Soffar, *PeerJ*, 2018, 2018, 1–17.
- 5 K. Elbanna, O. M. Sarhan, M. Khider, M. Elmogy, H. H. Abulreesh and M. R. Shaaban, *J. Food Drug Anal.*, **2017**, *25*, 667–680. **DOI:**10.1016/j.jfda.2017.01.005

<b>Table 1.</b> Results of SY and P4R	determination in model solutions	and soft drink $(n = 3, P = 0.95)$

Analyte	Sample	Spiked, µg/mL	Found, µg/mL	Recovery, %	RSD, %
Sunset Yellow FCF	Model solution	5	$4.75 \pm 0.45$	95	3.8
		2.5	$2.45 \pm 0.31$	98	5.1
		0.5	$0.48 \pm 0.08$	96	6.9
	Soft drink	5	$4.78 \pm 0.75$	96	6.3
		2.5	$2.41 \pm 0.43$	96	7.1
		0.5	$0.461 \pm 0.09$	92	7.8
Ponceau 4R	Model solution	5	$4.82 \pm 0.47$	96	3.9
		2.5	$2.51 \pm 0.3$	100	4.75
		0.5	$0.55 \pm 0.08$	110	5.9
	Soft drink	5	$4.68 \pm 0.63$	94	5.4
		2.5	$2.35 \pm 0.43$	94	7.3
		0.5	$0.53 \pm 0.11$	106	8.1

- 6 D. Bhatt, K. Vyas, S. Singh, P. J. John and I. Soni, *Food Chem. Toxicol.*, 2018, 113, 322–327. DOI:10.1016/j.fct.2018.02.011
- 7 H. Imane, S. Bellahcen and F. Souna, *Int. J. Pharm. Pharm. Sci.*, **2011**, *3*, 159–169.
- 8 H. Karimi-Maleh, H. Beitollahi, P. Senthil Kumar, S. Tajik, P. Mohammadzadeh Jahani, F. Karimi, C. Karaman, Y. Vasseghian, M. Baghayeri, J. Rouhi, P. L. Show, S. Rajendran, L. Fu and N. Zare, *Food Chem. Toxicol.*, **2022**, *164*, 112961. **DOI**:10.1016/j.fct.2022.112961
- 9 N. Vladislavić, M. Buzuk, I. Š. Rončević and S. Brinić, *Int. J. Electrochem. Sci.*, **2018**, *13*, 7008–7019.
- 10 K. Rovina, L. A. Acung, S. Siddiquee, J. H. Akanda and S. M. Shaarani, *Food Anal. Methods*, **2017**, *10*, 773–787. **DOI:**10.1007/s12161-016-0645-9
- 11 W. Zhang, T. Liu, X. Zheng, W. Huang and C. Wan, *Colloids Surfaces B Biointerfaces*, 2009, 74, 28–31.
  DOI:10.1016/j.colsurfb.2009.06.016
- 12 P. S. Dorraji and F. Jalali, *Food Chem.*, **2017**, *227*, 73–77. **DOI:**10.1016/j.foodchem.2017.01.071
- L. Zhao, F. Zhao and B. Zeng, *Electrochim. Acta*, 2014, 115, 247–254. DOI:10.1016/j.electacta.2013.10.181
- 14 Y. Songyang, X. Yang, S. Xie, H. Hao and J. Song, *Food Chem.*, **2015**, *173*, 640–644. **DOI**:10.1016/j.foodchem.2014.10.075
- 15 A. Chebotarev, K. Pliuta and D. Snigur, *Turkish J. Chem.*, **2018**, *42*, 1534–1543. **DOI:**10.3906/kim-1805-37
- 16 A. N. Chebotarev, K. V. Pliuta and D. V. Snigur, *ChemistrySelect*, **2020**, 5, 3688–3693. **DOI:**10.1002/slct.202000518
- 17 K. Pliuta and D. Snigur, *Anal. Sci.*, **2022**, *38*, 1377–1384. **DOI:**10.1007/s44211-022-00170-y
- 18 Y. Zhang, X. Zhang, X. Lu, J. Yang and K. Wu, Food Chem., 2010, 122, 909–913. DOI:10.1016/j.foodchem.2010.03.035
- 19 R. A. Medeiros, B. C. Lourencao, R. C. Rocha-Filho and O. Fatibello-Filho, *Talanta*, **2012**, *99*, 883–889. **DOI:**10.1016/j.talanta.2012.07.051
- 20 B. Allen J. and F. Larry R., Eletrochemical methods: Fundamental and applications, 2004, vol. 677.
- 21 S. V. Kurkov and T. Loftsson, *Int. J. Pharm.*, **2013**, *453*, 167–180. **DOI:**10.1016/j.ijpharm.2012.06.055
- 22 T. Ogoshi and A. Harada, Sensors, 2008, 8, 4961–4982.
  DOI:10.3390/s8084961
- 23 A. Yilmaz, E. Yilmaz, M. Yilmaz and R. A. Bartsch, *Dye. Pigment.*, 2007, 74, 54–59. DOI:10.1016/j.dyepig.2006.01.011
- 24 E. Y. Ozmen, M. Sezgin, A. Yilmaz and M. Yilmaz, *Bioresour. Technol.*, 2008, 99, 526–531.
  DOI:10.1016/j.biortech.2007.01.023

- B. Hosangadi and S. Palekar, J. Incl. Phenom. Mol. Recognit. Chem., 1989, 7, 321–325. DOI:10.1007/BF01076985
- 26 M. Suzuki, Y. Sasaki and M. Sugiura, Chem. Pharm. Bull., 1970, 8, 1797–1805.
- 27 Y. Li, Y. Li, L. Jia, Y. Li, Y. Wang, P. Zhang and X. Liu, J. Iran. Chem. Soc., 2021, 19, 1251–1260.
  DOI:10.1007/s13738-021-02375-w
- 28 D. V. Snigur, A. N. Chebotarev and K. V. Bevziuk, *J. Appl. Spectrosc.*, 2018, 85, 21–26.
  DOI:10.1007/s10812-018-0605-9
- 29 K. Bevziuk, A. Chebotarev, A. Koicheva and D. Snigur, *Monatshefte fur Chemie*, **2018**, *149*, 2153–2160. **DOI:**10.1007/s00706-018-2301-0
- 30 X. Qin and X. Zhu, Anal. Lett., 2016, 49, 189–199. DOI:10.1080/00032719.2015.1065880
- 31 G. M. D. Ferreira, G. M. D. Ferreira, M. C. Hespanhol, J. de Paula Rezende, A. C. dos Santos Pires, L. V. A. Gurgel and L. H. M. da Silva, *Colloids Surfaces A Physicochem. Eng. Asp.*, 2017, 529, 531–540. DOI:10.1016/j.colsurfa.2017.06.021
- 32 D. K. Gosser, Cyclic Voltammetry: Simulation and Analysis of Reaction Mechanisms, New York, **1994**.
- 33 E. Laviron, J. Electroanal. Chem., 1979, 101, 19–28. DOI:10.1016/S0022-0728(79)80075-3
- 34 R. H. Wopschall and I. Shain, Anal. Chem., 1967, 39, 1535– 1542. DOI:10.1021/ac50156a020
- 35 Y. Zhang, L. Hu, X. Liu, B. Liu and K. Wu, Food Chem., 2015, 166, 352–357. DOI:10.1016/j.foodchem.2014.06.048
- 36 A. Chebotarev, A. Koicheva, K. Bevziuk, K. Pliuta and D. Snigur, *J. Food Meas. Charact.*, **2019**, *13*, 1964–1972. **DOI:**10.1007/s11694-019-00115-6
- 37 P. Sierra-Rosales, C. Berríos, S. Miranda-Rojas and J. A. Squella, *Electrochim. Acta*, 2018, 290, 556–567.
  DOI:10.1016/j.electacta.2018.09.090
- 38 S. Combeau, M. Chatelut and O. Vittori, *Talanta*, **2002**, *56*, 115–122. **DOI:**10.1016/S0039-9140(01)00540-9
- 39 S. Momeni and D. Nematollahi, Sci. Rep., 2017, 7, 1–10. DOI:10.1038/s41598-017-04581-0
- 40 D. Yang, L. Zhu and X. Jiang, *J. Electroanal. Chem.*, **2010**, 640, 17–22. **DOI:**10.1016/j.jelechem.2009.12.022
- 41 Eurachem, The Fitness for Purpose of Analytical Methods: A Laboratory Guide to Method Validation and Related Topics, 2014
- 42 S. Ellison, V. Barwick and T. Duguid Farrant, *Practical Statistics for the Analytical Scientist*, RSC Publishing, London, 2nd edn., **2009**.

#### Povzetek

Ena od slabih strani voltametrijske analize je znatna količina vzorca, potrebnega za elektrolizo v celici. V članku za rešitev tega problema predstavljamo metodologijo, podobno adsorpcijski inverzni (stripping) voltametriji, za analizo dveh azo barvil – Sunset Yellow FCF in Ponceau 4R. Za delovno elektrodo predlagamo elektrodo iz ogljikove paste, modificirano z  $\beta$ -ciklodekstrinom, cikličnim oligosaharidom, ki lahko tvori supramolekularne komplekse z azo barvili. Preučili smo redoks obnašanje barvil Sunset Yellow FCF in Ponceau 4R: število elektronov in protonov ter koeficiente prenosa naboja na predlagani senzor. Pogoje za določevanje obeh barvil smo optimizirali z uporabo voltametrije pravokotnih pulzov (square-wave). Pri optimalnih pogojih so bile umeritvene krivulje linearne v območju 71–565  $\mu$ g/L za Sunset Yellow FCF in 189–3024  $\mu$ g/L za Ponceau 4R. Na koncu smo novi senzor preizkusili za določitev Sunset Yellow FCF in Ponceau 4R v brezalkoholnih pijačah z voltametrijo pravokotnih pulzov. Vrednosti RSD so bile največ 7,8 in 8,1 %, kar je zadovoljiva ponovljivost za oba analizirana vzorca.



Except when otherwise noted, articles in this journal are published under the terms and conditions of the Creative Commons Attribution 4.0 International License